Nonlinear processes in led tungstate crystal under two-photon interband laser excitation.

Authors:

V. I. Lukanin

A. Ya. Karasik

Affiliations:

Prokhorov General Physics Institute, Russian Academy of Sciences, 38 Vavilov str., Moscow, 119991 Russia

Correspondence author:

A. Ya. Karasik

E-mail: karasik@lst.gpi.ru

ABSTRACT

Dynamics of interband two-photon absorption (TPA) in crystals excited by a sequence of 25 picosecond laser pulses and 450-700 nm continuous probe radiation is analyzed. Trains of pulses of second (523.5 nm), third (349 nm) and fourth (262nm) harmonics of 1047 nm Nd:YLF laser were used for interband TPA in crystals. Induced absorption (IA) from excited by TPA electronic levels has been revealed and kinetics of the IA reflects the dynamics of energy migration between neighboring tungstate ions to traps. The increase in the laser pump repetition rate leads to the long-lived accumulation of electronic excitations. The control of pump repetition rate and the number of excitations increase IA relaxation time more than two orders of magnitude. The relaxation time of IA at 10K exceeds 100 min. Under accumulated due to TPA electronic excitations in the $PbWO_4$ crystal at 10 K, the intrinsic luminescence decay time exceeds 45 min.

1. Introduction

Processes concerning the generation and relaxation of electronic excitations in inorganic [1] and organic [2] media are of particular interest. Methods of laser spectroscopy are widely used for investigations of basic properties of materials and interaction of light with matter. In this respect the nonlinear two-photon absorption (TPA) technique attracts attention due to a number of unique properties. The TPA technique is applicable to control the energy, time, spectral, and spatial parameters of laser radiation [3]. In addition, the TPA technique makes it possible to increase the spatial resolution in laser microstructuring of materials and microscopy. The list of TPA applications can be significantly extended [2].

Two-photon nonlinear spectroscopy can provide new information that is inaccessible by traditional one-photon spectroscopy [4, 5]. The use of the TPA technique is advantageous, in particular, for excitation of electronic states in the conduction band of materials. For one-photon excitation in nontransparent spectral range of the conduction band large nonradiative losses do not give a possibility to obtain bulk homogeneous excitation of a sample [6]. In the case of interband TPA, the energy of one of the excitation photons can correspond to the transparency region of the material. There appears the possibility to get rid of nonradiative losses in the near-surface layer of the material, which depend on the surface quality and dramatically distort the spectra and decrease the real quantum yield of the luminescence [6].

In this case, selective laser excitation of levels under TPA can allow direct examination of luminescence and absorption from the interior of a bulk sample. The difference between the selection rules for one- and two-photon excitation processes provides additional capabilities. The measurement of the TPA coefficients and cross-sections are of independent interest.

The optical properties of oxide tungstate and molibdate crystals are of current interest because of the use of these crystals in scintillation detector of ionizing radiation [1], in addition to their promising use as nonlinear optical materials, e.g., as shifters of a laser radiation frequency via stimulated Raman scattering (SRS) [7]. Applications of the crystals require knowledge of the scintillation response rate. As a rule this rate is measured using methods of the one-photon fluorescence spectroscopy. However, a search of new methods for investigations of dynamics of generation and relaxation of electronic excitations is important. In [9], we demonstrated a method to analyze the dynamics of interband TPA in tungstate crystals excited by a sequence of picosecond laser pulses of variable intensity while under continuous probe radiation. We measured the TPA coefficients for several tungstates and molibdates and analyzed the competition between TPA and SRS [10].

2. Experimental methods

In this work, we modernized the experimental scheme used in [10]. The crystals were excited by the second (532.5 nm), third (349 nm), and fourth (262 nm) harmonics of a passively mode-locked and Q-switched Nd:$YLiF_4$ laser. We increased a cavity length and respectively laser axial interval to 15 ns for more exact measurement kinetics of fluorescence decay in nanosecond time scale.

The interband absorption edge of the PWO crystal, which we studied in this

paper more carefully in particular, extends from ~330 nm, and the energy of one of the excitation photons (λ = 523.5 and 349 nm) lies inside the crystal transparency range, while the sum of the energies of these two photons (4.74 or 7.1 eV) corresponds to the conduction band of the crystal. (The band gap width of the crystal, according to different sources, lies within the range 3−4.7 eV (see [10] and references therein).) The TPA coefficients of PWO crystal, depending on the direction of the linear polarization of the excitation radiation, vary within 0.6−1.2 cm/GW for the wavelength 523.5 nm and within 1.5–1.6 cm/GW for λ = 349 nm [10]. A single-mode radiation (trains of pulses with a duration of 25 ps, an energy up to 3 mJ, and a repetition rate up to 10 Hz) was focused by a lens with f = 112 mm into the 28 mm long studied crystal, which had the form of a parallelepiped with polished surfaces. To measure the luminescence spectra and kinetics, the emission from a lateral face of the crystal was collected by a lens and directed to the PMT (FEU-136 or FEU-87), whose signal was analyzed by a Tektronix DPO 4104 oscilloscope with a bandwidth of 1 GHz. The luminescence spectrum was measured using an Ocean Optics USB4000 spectrometer. The crystal was cooled in a closed-cycle helium cryostat.

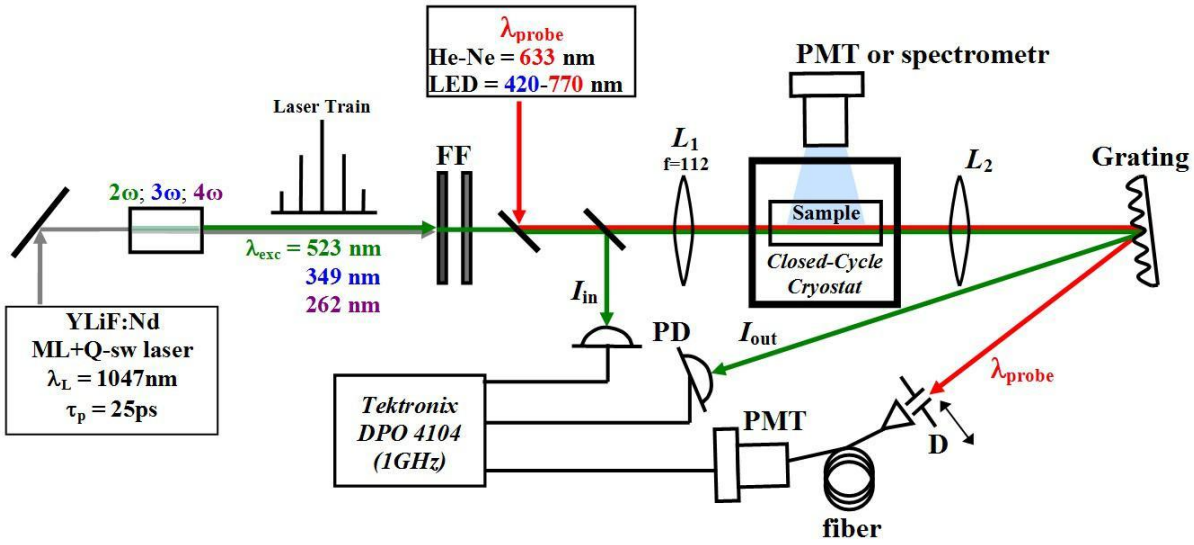

Figure 1. Schematic of the experimental setup.

3. Experimental results

3.1. Dynamics of induced absorption at the probe light frequency

Figure 2 shows the kinetics of the probe light intensity, measured with the photoelectron multiplier during crystal excitation by high-power picosecond radiation for the case where the diaphragm centre is aligned with the pump and probe beam axes (Fig.1). It follows from the oscillograms in Fig. 2 that, after the crystal excitation, pulses with duration of ~ 0.5 ms arise in the kinetics of cw He–Ne laser radiation. The pulse frequency was equal to the repetition rate of picosecond excitation trains, which was varied within 0.1 – 10 Hz. For focusing lens with f = 112 mm, the 'positive' pulse amplitude in Fig. 2 was larger by a factor of 3 – 4 than for the case where the lens with a longer focal length (f = 250 mm) was used (i.e., at a

lower excitation intensity and weaker crystal heating). The pump spot radius in the lens focus (f =112 mm) was 16 μm (at the $1/e^2$ level), the beam waist length was 6 mm, and the probe light spot radius was 80 μm at a probe power of 8 μW (for the lens with f = 250 mm, the pump spot radius in the focus was 36 m and the beam waist length was 30 mm).

The oscillogram in Fig. 2 also exhibits a 'negative' spike with a relaxation time of several tens of milliseconds. The oscillogram recorded with the diaphragm displaced from the probe beam centre by a distance exceeding the diaphragm diameter (4 mm) contains only a negative spike (Figs 2, 3), which was explained by us in [8] as the result of one-photon absorption on the transitions from the electron levels excited due to two-photon absorption to the trap (defect) levels.

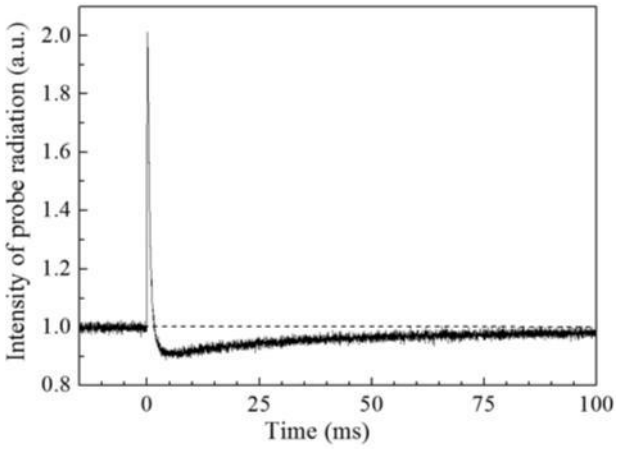

Figure 2. Oscillogram of the probe radiation during $PbWO_4$ crystal excitation by a train of pulses (λ_{exc} = 523.5 nm, ***E***||C4, ***k*** C4) for the case where the diaphragm centre is aligned with the beam axes.

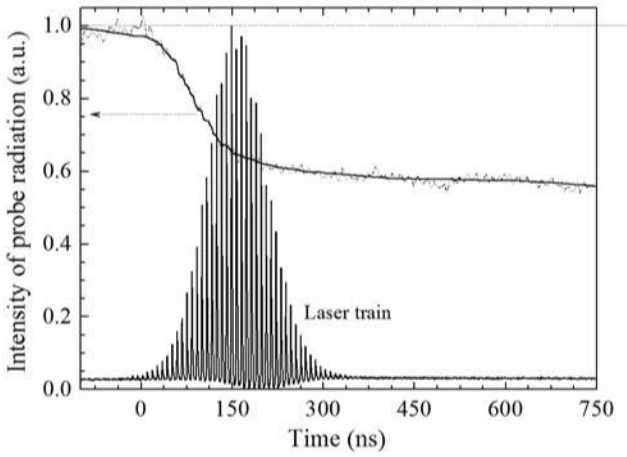

Figure 3. Oscillogram illustrating the kinetics of induced absorption during $PbWO_4$ crystal excitation (λ_{exc} = 523.5 nm, ***E***||C4, ***k*** C4) by a train of pulses, when diaphragm D (Fig. 1) is displaced from the probe beam center by a distance exceeding its diameter.

Note that the induced absorption is initiated even by the first, relatively weak excitation train pulses (Fig. 3). In the beginning of induced absorption pulse, one can observe a stage of rapid exponential rise with a rise constant of ~ 60 ns, which is followed by a stage of relatively slow rise with a characteristic time of ~10 ms assigned by us to the migration of electronic excitation to crystal defects (traps) and, finally, an excitation relaxation stage (Fig. 2) with a characteristic relaxation time of ~ 100 ms. A replacement of the probe light source having a wavelength 633 nm with a 532 nm laser did not change much the oscillogram shape.

We verified if the positive pulse in the oscillogram presented in Fig. 2 indicates the predicted in [11, 12] probe light amplification. Measurements of the probe light energy at the crystal input and output showed that the amplification is absent and that the pulses arise in the cw radiation spectrum due to the generation of a thermal lens in the crystal and, as a consequence, beam focusing (Fig. 4).

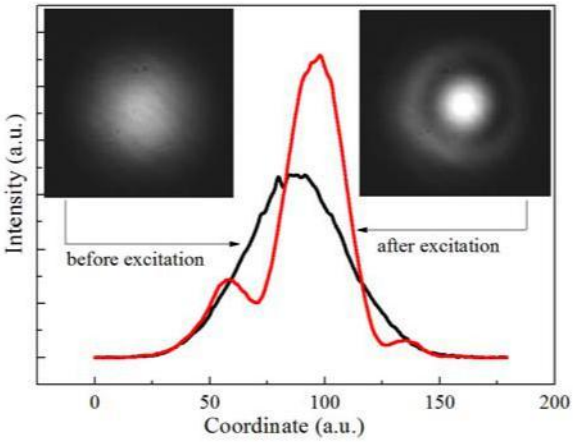

Figure 4. Formation of a thermal lens in a $PbWO_4$ crystal under picosecond pumping with λ_{exc} = 523.5 nm. The insets show the probe beam profiles before and after the crystal excitation.

3.2. Crystal for accumulation of laser energy

For investigation of the kinetics of the induced absorption from a level excited by TPA, we directed a cw probe beam of a He-Ne laser with λ = 633 nm and a power of ~1 mW into the crystal collinearly with the picosecond excitation beam (Fig. 1). The use of probe radiation allows us to study the dynamics of induced absorption from the excited state in a wide spectral and temporal range.

Figure 5 shows the rise kinetics of the absorption induced by accumulation of electronic excitations upon TPA in the PWO crystal at the temperature T = 10 K. The kinetics was measured at the 633 nm probe beam wavelength with the pump laser wavelength 523.5 nm at the laser flash pulse repetition rate of 2Hz.

In the first stage of the kinetics, the induced absorption rapidly grows and the absorbed energy is accumulated in the paraxial region of laser excitation (Fig. 5b). As a result, after several excitation pulses, the induced absorption slightly

changes with the increasing number of excitation pulses. In this process, the transmission at the probe wavelength (I_{out}/I_{in}) decreases practically from 0. This induced absorption located in the paraxial region of the crystal is the reason for the creation of thermal lens. After switching off the laser excitation, the absorption slowly decays with a relaxation time exceeding 100 min (Fig. 6).

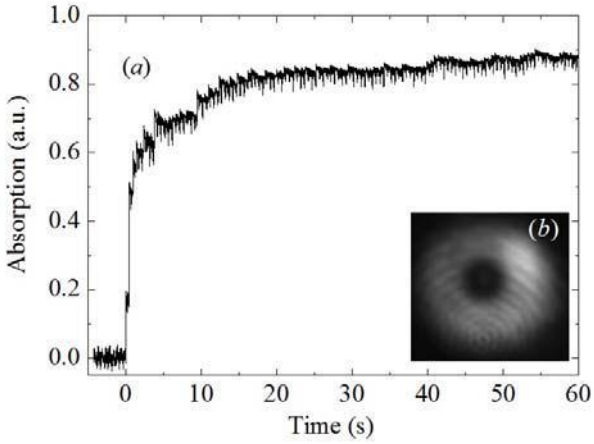

Fig. 5. Rise kinetics of the absorption induced by accumulation of electronic excitations upon interband two-photon absorption in the $PbWO_4$ crystal at the temperature T = 10 K. The kinetics was measured at the 633 nm probe beam wavelength with the pump laser wavelength 523.5 nm at a pulse repetition rate of 2 Hz (*a*). Image of a probe beam cross section after two-photon absorption at the exit from the crystal and accumulation of electronic excitations (*b*).

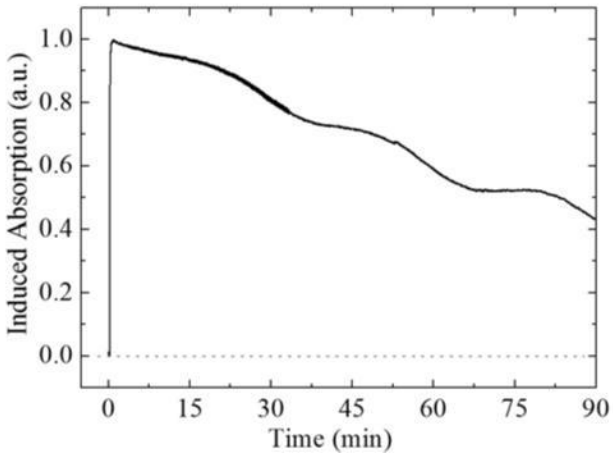

Fig. 6. Decay kinetics of induced absorption after interband two-photon absorption and accumulation of electronic excitation in the $PbWO_4$ crystal at T = 10 K measured at the 633 nm probe wavelength.

We also used as a probe beam a radiation of a pigtailed white LED with a broadband spectrum extending from ~450 to 750 nm (Fig. 7a). Under two-photon laser excitation, the induced absorption of broadband probe radiation reaches a maximum value, which is comparable with that for the monochromatic 633 nm probe radiation. The induced broadband absorption (transmission) practically does not depend on wavelengths in the 450–750 nm spectral range (Fig. 7b). We can explain this effect of induced broadband absorption by the fact that, after TPA and one-photon absorption from the excited state, the excitations can be delivered to defect centers or traps via the direct transition between the excited and trap levels or via excitation migration between these levels [8]. The spectrum of the traps could be continuous and accordingly broad. (The electronic state excited by TPA could also be energetically broadened.) Relatively uniform distribution of occupied trapping sites with preferential occupation of the deepest traps could take place [13].

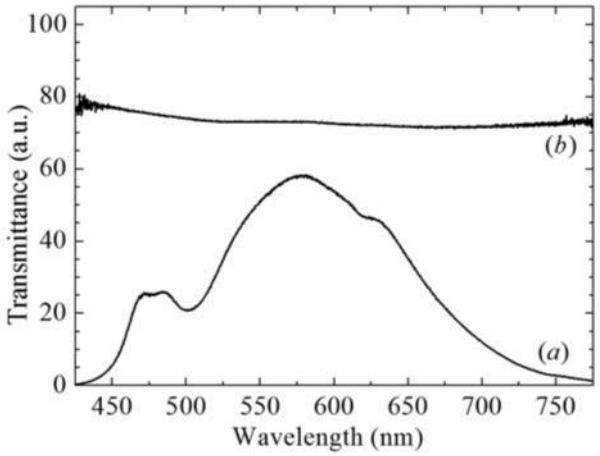

Fig. 7. Broadband spectrum of the LED (*a*). Broadband transmission spectrum induced by two-photon laser excitation of $PbWO_4$ crystal at T = 10 K (*b*)

We have supposed that the electronic energy accumulated in the crystal as a result of TPA, which is concentrated in a limited volume of the crystal and, hence, has a relatively high density, must lead to the excitation of the intrinsic luminescence of the crystal. (The sum energy of two green excitation photons - 4.74 eV falls into the high-energy wing of the luminescence excitation spectrum [6] and thus must excite the intrinsic luminescence of the crystal). For this purpose, we used 523.5 nm laser excitation of the crystal at T = 10 K. For excitation and energy accumulation, the laser with a pulse repetition rate of 5 Hz was switched on for a time shorter than 5 sec and then was switched off. After switching off the laser, we registered the luminescence emission, which was clearly visually seen at short times. Figure 8(*a*,*b*) demonstrates the intrinsic luminescence decay kinetics with a decay time exceeding 2000 sec under T=10K. (The inset in Fig. 8(*b*) shows the luminescence decay kinetics at the initial stage.) The increase temperature of the sample from helium to room temperature leads to sharp increase in temporal resolution from ~100 ns to ~2 ns (Fig.8 (*b*), (*c*)).

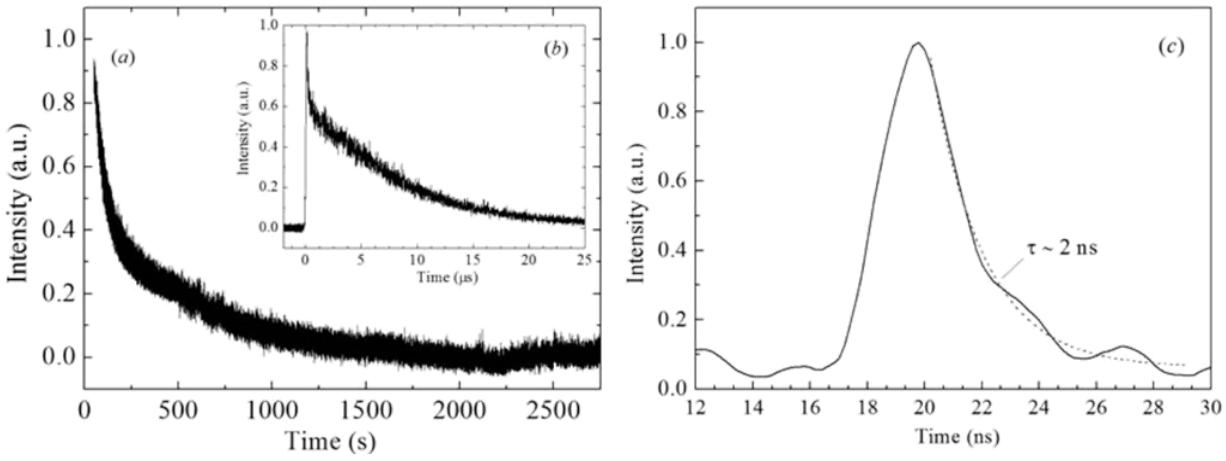

Fig. 8. Decay kinetics of the intrinsic luminescence in a $PbWO_4$ crystal under T=10K (*a*, *b*) and T=300K (*c*) excited by the energy accumulated due to the interband two-photon absorption (measured after switching off the laser excitation). The inset (*b*) shows the luminescence decay kinetics at the initial stage at 10K.

Note that the intrinsic luminescence of excited PWO crystals was studied in a number of works, which is related to the use of these crystals in detectors of ionizing radiation and in scintillators [1, 4, 14-20]. In the above-cited studies, the structure of the intrinsic luminescence spectra of PWO crystals was determined using different luminescence excitation methods, including UV, X-ray, synchrotron radiation and one- and two-photon laser excitation [20]. In [20], the blue luminescence was ascribed to the radiative decay of self-trapped excitons, which locate at regular tungstate molecules.

In general, the spectra excited by TPA resemble the spectra measured by other methods. The spectra include a short-wavelength (blue) band at $\lambda \sim 420–425$ nm and a long-wavelength (green-red) band at $\lambda \sim 500–600$ nm. The blue band is assumed to belong to the intrinsic luminescence of $(WO_4)^{2-}$ (or excitons) molecular ions of the regular crystal lattice, while the green-red band is related to the presence of (WO_3) groups in combination with F color centers in the crystal [6]. Figure 9 shows the luminescence spectra measured by us at T = 10 K upon two-photon excitation with λ = 523.5 nm and λ = 349 nm and upon relatively low-power one-photon excitation at λ = 262 nm.

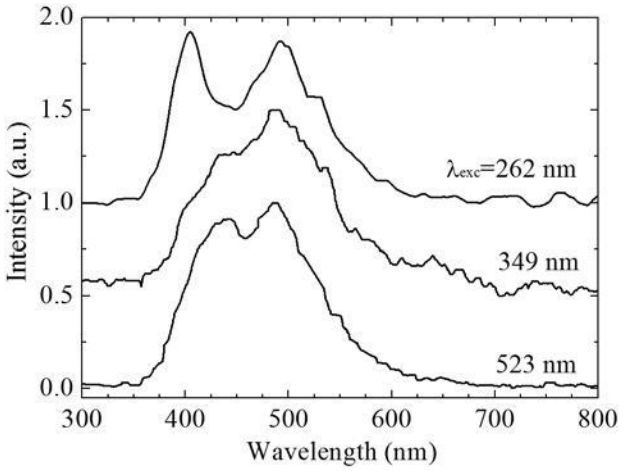

Fig. 9. Luminescence spectra of a PbWO4 crystal (T = 10 K) upon interband two-photon laser excitation with = 523.5 and 349 nm and single-photon excitation with = 262nm.

In Fig. 9, one can see some difference in the positions and intensities of the bands in the spectra measured upon two- and one-photon excitation of the crystal. In particular, the measured at 262 nm one-photon excitation blue band of the intrinsic luminescence is shifted to shorter wavelengths (to 400 nm) relatively to the spectra excited by TPA. This circumstance can be related to different selection rules for OPA and TPA, but this suggestion should be confirmed by additional studies.

We were able to reliably measure intrinsic luminescence spectra excited by TPA in PWO crystal only in the 10−77 K temperature range. At room temperature, the luminescence was quenched and the signal was too weak for reliable recording. It was shown in paper [6] that the luminescence excitation spectrum intensity (or the number of excited optical centers) for PWO crystal decreases quite sharply as temperature rises from helium to room temperature. Another situation is for some tungstate and molybdate crystals (for example, $ZnWO_4$ or $CaMoO_4$), where the luminescence spectra at TPA are well measured in the entire 10–300 K temperature range.

4. Conclusion

The picosecond two-photon interband laser excitation of PbWO4 crystal at a temperature of 10 K leads to electronic excitation energy accumulation, which results in almost 100% induced absorption in the 450−750 nm spectral range. Effect of the creation of thermal lens is explained by local heating of the crystal under two-photon laser irradiation by focused paraxial laser beam. This high induced absorption located in local paraxial region of the crystal is the reason of creation of thermal lens. The relaxation time of this induced absorption exceeds 100 min. The electronic excitation energy accumulated in the PWO crystal at T = 10 K excites the intrinsic luminescence with a decay time longer than 45 min, which is comparable with the relaxation time of the accumulated electronic excitation energy. We also measured the decay kinetics and the spectra of the intrinsic luminescence of the PWO crystal at a temperature of 10 K under two-photon and one-photon excitation and revealed differences in the structure of the spectra.

ACKNOWLEDGMENTS

This work was supported by the Russian Foundation for Basic Research (project no. 16-02-00338) and the Russian Scientific Foundation (project no. 14-22-00248).

References

1. M. Nikl, phys. stat. sol. (a) **178**, 595 (2000).
2. M. Rumi and J.W. Perry, Advances in Optics and Photonics **2** (4), 451 (2010).
3. V.V. Arsenyev, V.S. Dneprovskii, D.N. Klyshko, and A.N. Penin, Sov. Phys. JETP **29** (3), 413 (1969).
4. W. Kaiser, C.G.B. Garret, Phys. Rev. Lett. **7** (6), 229 (1961).
5. V.B. Mikhailik, H. Kraus, D. Wahl, M. Itoh, M. Koike, I. K. Bailiff, Phys. Rev. B **69**, 205110 (2004).
6. J.A. Groenik and G. Blasse, J. Solid State Chem. **32** (1), 9 (1980).
7. T.T. Basiev, P.G. Zverev, A.Ya. Karasik, V.V. Osiko, A.A. Sobol', and D.S. Chunaev, JETP **99** (5), 934 (2004).
8. V. I. Lukanin and A. Ya. Karasik, JETP **117**, 198 (2013).
9. V.I. Lukanin, D.S. Chunaev, and A.Ya. Karasik, JETP Lett. **91** (11), 548 (2010).
10. V. I. Lukanin and A. Ya. Karasik, Opt. Commun. **336**, 207 (2015).
11. A.M.Prokhorov *Usp. Fiz. Nauk*, **85**, 599 (1965).
12. A.M. Prokhorov *Science*, **10**, 828 (1965).
13. R. L. Fork, C. V. Shank, A. M. Glass, A. Migus, M. A. Bosch, and J. Shah, Appl. Phys. Lett. **43**, 394 (1979)
14. M. Nikl, K. Nitsch, and K. Polak, Phys. Status Solidi B **195**, 311 (1996).
15. G. Tamulaitis, S. Buracas, and V. P. Martinov, Phys. Status Solidi A **157**, 187 (1996).
16. A. Annenkov, E. Auffray, and M. Korzhik, Phys. Status Solidi A **170**, 47 (1998).
17. W. van Loo, Phys. Status Solidi A **27**, 565 (1975).
18. D. Millers, L. Grigorjeva, and S. Chernov, Phys. Status Solidi B **203**, 585 (1997).
19. A.A. Blistanov, B.I. Zadneprovskii, and M.A. Ivanov, Crystallogr. Rep. **50**, 284 (2005).
20. M Itoh, M Horimoto and M Fujita J. Phys.: Condens. Matter 15, 193 (2003)

